

## Modeling the Process of Hillslope Soil Erosion in the Loess Plateau

T. J. Li, G. Q. Wang\*, Y. F. Huang, and X. D. Fu

*State Key Laboratory of Hydrosience and Engineering, Tsinghua University, Beijing 100084, China*

Received 30 September 2008; revised 9 July 2009; accepted 21 July 2009; published online 10 September 2009

**ABSTRACT.** High-peak short-duration surface runoff is the primary cause of severe soil erosion and hyper-concentrated sediment-laden flow in the Loess Plateau of China. This paper proposed a model to simulate the process of hillslope soil erosion in the Loess Plateau, which is essential to support environmental friendly land use and conservation policies. Infiltration excess runoff in this region is simulated by calculating the infiltration rate of land surface in each hillslope unit. The time series of surface runoff are used as the input to simulate soil erosion process with the same time step of several minutes. A dimensionless equation with obvious physical basis is proposed to quantify the amount of erosion according to the runoff. Two parameters denoting soil erodibility and microtopography are raised in the equation and are proved reasonable by experimental data. The parameters are further calibrated and validated using data from field plots. At last, satisfiable results are achieved when used the model with continuous rainfall data from a watershed in the Loess Plateau, by which the proposed hillslope soil erosion model is approved playing a crucial part in building up a comprehensive watershed model.

*Keywords:* erodibility, infiltration, Loess Plateau, microtopography, soil erosion modeling, the Yellow River

### 1. Introduction

The Loess Plateau, the center of loess deposits with an area of about 630,000 km<sup>2</sup>, lies in the arid and semi-arid region in the Northwest China. This region has the typical monsoon climate with an annual precipitation of 150~700 mm. However, the potential evaporation can reach as high as 1400~2000 mm. Precipitation primarily occurs in summer and early fall seasons with high-peak short-duration characteristics. The amount of soil erosion resulted from intensive surface runoffs generated during those storms contributes over 70% of annual sediment yield. There are mainly two aspects contributing to the complexity and uniqueness of soil erosion processes in the Loess Plateau. One is that sediment concentration in this highly erodible region can easily reach 1,000 kg/m<sup>3</sup>, which rarely happens in other river basins. The other is that the steep slope of hillslopes exceeds the assumption of gentle slope in most erosion models for farmland and rangeland. Soil erosion in steep hillslopes is caused by not only water flow but also gravity. Namely, collapse and landslide frequently happen in gully region and lead to notable gravitational erosion amount.

Many researchers have developed various statistical soil erosion models through regression analysis of data from cer-

tain subbasins of the middle Yellow River basin. For example, Li et al. (1998) proposed relationships between flood discharge and sediment concentration of the Kuye River. Cai et al. (2004) set up a model to estimate soil erosion amount of each storm event of the Chabagou watershed. However, the amount of soil erosion highly depends on the temporal and spatial distribution of rainfall, but those statistical models do not reproduce the whole process of soil erosion, which makes the estimation of erosion amount somewhat unreliable. Furthermore, if a soil erosion model does not run on a fine temporal resolution, it is incapable of being integrated into a comprehensive watershed model. That is because non-equilibrium sediment transport in river network, which not only carries sediment particles but also deposits them or entrains more sediment in water flow, is generally dynamically simulated after soil erosion.

Although physically-based soil erosion models, such as CREAMS (Knisel, 1980), WEPP (Flangan and Nearing, 1995), and ANSWERS-2000 (Dabral and Cohen, 2001), overcame most weaknesses of statistical models. But they are not widely used for the soil erosion process in the Loess Plateau of China due to two reasons. Firstly, the development of upland rills and gullies in the Loess Plateau are more extensive and intensive than the rill space assumption in those models. Secondly, high sediment load in runoff in the Loess Plateau may increase the detachment rate in rills rather than that of weakening assumed in those models (Foster and Meyer, 1972).

In virtue of the development of information technologies, such as Remote Sensing (RS) and Geographical Information

\* Corresponding author. Tel.: +86 10 62781748; fax: +86 10 62772463.

E-mail address: dhwgq@tsinghua.edu.cn (G. Q. Wang).

System (GIS), river basins are expected to be delineated and simulated digitally. Wang et al. (2007) developed a framework of watershed modeling for the Yellow River, namely the Digital Yellow River Model (DYRIM). The DYRIM takes the advantages of digital elevation model (DEM), drainage network codification (Li et al., 2009), RS- and GIS-based parameter acquisition, and parallel computing to facilitate physically-based, distributed-parameter and continuous simulations of hydrological, soil erosion and sediment transport processes in river basins. The DYRIM is designed to comprise a rainfall-runoff model for hillslopes, a hydraulic soil erosion model for hillslopes, a gravitational erosion model for gully region, and a non-equilibrium sediment transport model for channels.

The first version of the hillslope soil erosion model that meets the demand of DYRIM is briefly introduced by Wang et al. (2007). That erosion model takes the time series of surface runoff as its input to obtain the detailed process of soil erosion with the same time step as runoff, but the parameters in that model are not carefully investigated. This paper proposes an improved version of the hillslope soil erosion model. Two parameters denoting soil erodibility and the microtopography of hillslope respectively are clearly introduced and verified using experimental data in this paper. For application, the proposed model is integrated in the framework of the DYRIM and is applied to the Chabagou watershed to prove its validity.

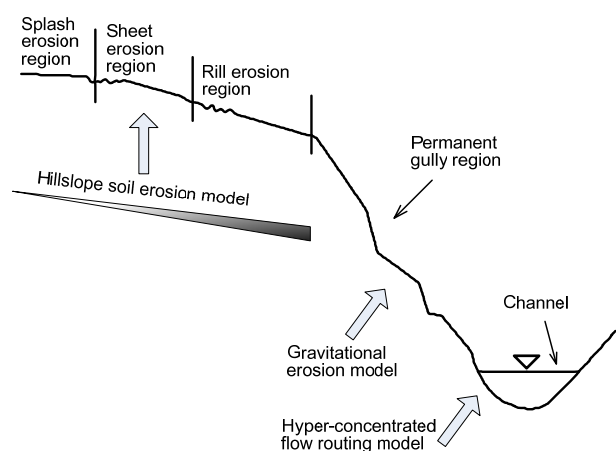


**Figure 1.** Modeling schematic of the soil erosion and sediment transport processes in the Loess Plateau of China [adopted from Li (2008)].

## 2. The Hillslope Soil Erosion Model

Splash erosion, sheet erosion and rill erosion are conceptualized to a general process of hillslope soil erosion in this study as shown in Figure 1. By assuming that the erosion process occurs uniformly in the contour direction, it reduces to a one-dimensional process along the hillslope. In this paper, the time series of surface runoff are used as the input to estimate the amount of soil erosion at each time step. The influences of factors such as soil property, slope, roughness, and vegetation co-

ver to soil erosion and rainfall-runoff processes are considered separately through introducing a set of physical parameters into the models.

The dot-filled part in Figure 2 is a basic unit to illustrate the soil erosion process. In Figure 2, variable  $x$  denotes the distance from the top of the hillslope, and  $\Delta x$  denotes the length of the basic unit along the hillslope. In this paper, it is assumed that among all the sediment particles passing the observation section,  $m_x \cdot \Delta x$  layers of them are newly detached from the basic unit. That is, the eroding rate is  $m_x$  layers of particles per meter along the hillslope.

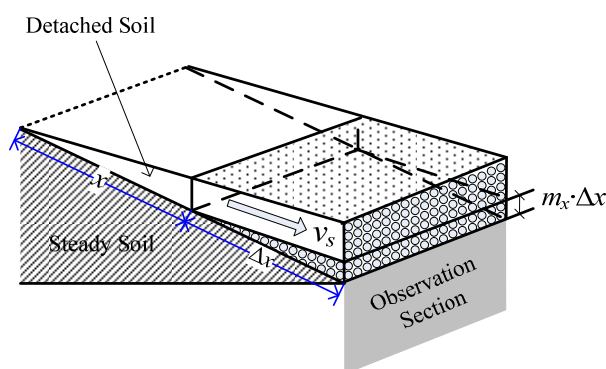


**Figure 2.** A basic unit (the dot-filled part) on the surface of a conceptual hillslope for the illustration of soil erosion process.

In order to quantify the mass of newly detached sediment particles, in this paper the thickness of one layer of particles is assumed to be equal to the median diameter  $D$  of the particles. Thus, the mass of particles per layer per square meter is  $(1 - \theta_{us}) \cdot D \rho_s$ , where  $\rho_s$  is the density of sediment particles ( $\text{kg} \cdot \text{m}^{-3}$ ), and  $\theta_{us}$  is the porosity of the surface soil ( $\text{m}^3/\text{m}^3$ ) and equals to the saturated volumetric water content.

Therefore, soil erosion rate, namely the amount of soil detached per square meter per second, can be calculated in the way in this paper as:

$$e_x = (1 - \theta_{us}) m_x D \rho_s v_s \quad (1)$$

where  $e_x$  is in  $\text{kg} \cdot \text{m}^{-2} \cdot \text{s}^{-1}$ ;  $m_x$  is in  $\text{m}^{-1}$ ;  $v_s$  is the velocity of particles ( $\text{m} \cdot \text{s}^{-1}$ ) and is estimated as:

$$v_s = \alpha v \quad (2)$$

where  $\alpha$  is a coefficient smaller than 1;  $v$  is the velocity of the water flow ( $\text{m} \cdot \text{s}^{-1}$ ).

In sheet flow, hydraulic radius equals to runoff depth. According to the Manning's equation,  $v$  is calculated as:

$$v = h^{2/3} J^{1/2} / n \quad (3)$$

where  $n$  is the Manning's coefficient;  $h$  is the runoff depth (m);

and  $J$  is the slope of hillslope.

Flow discharge per meter width at position  $x$ , which is known from the rainfall-runoff model, is denoted as  $q_x$  and equals to  $vh$ .  $q_x$  is used to eliminate  $h$  from Equation (3), and thus  $v$  is solved as:

$$v = q_x^{2/5} n^{-3/5} J^{3/10} \quad (4)$$

By putting Equations (2) and (4) into Equation (1),  $e_x$  can be determined as:

$$e_x = (1-\theta_{us}) \alpha m_x D \rho_s q_x^{2/5} n^{-3/5} J^{3/10} \quad (5)$$

To describe the dynamics of soil erosion, in this paper  $m_x$  is proposed to be correlated to flow strength and the erodibility of surface soil as:

$$m_x D = k \Theta_x^\beta \quad (6)$$

where  $k$  is the coefficient related to the erodibility of surface soil,  $\Theta_x$  is the Shields parameter denoting the strength of flow at the position  $x$ ,  $\beta$  is the index related to the eroding efficiency of runoff. All those parameters are dimensionless.

According to the study of sediment incipient motion in river channels (Cao et al., 2006), the value of the index  $\beta$  can be determined by fluid and sediment characteristics. However, microtopography has significant impact on the convergence of flow on hillslope surface. The concentrated flow, e.g. in rills, can erode more particles than sheet flow. Therefore, microtopography is crucial to determine the amount of soil erosion, and should be taken as the main factor determining the exponent (i.e. the parameter  $\beta$ ) on flow strength.

The Shields parameter in Equation (6) is expressed as:

$$\Theta_x = \frac{\rho_m}{\rho_s - \rho_m} \frac{hJ}{D} \quad (7)$$

where  $\rho_m$  is the density of sediment laden flow ( $\text{kg}\cdot\text{m}^{-3}$ ). Replacing  $h$  by  $q_x/v$  in Equation (7) and then putting it into Equation (6) lead to:

$$m_x D = k \left( \frac{\rho_m}{\rho_s - \rho_m} \right)^\beta q_x^{3/5} n^{3/5} J^{7/10} D^{-\beta} \quad (8)$$

Putting Equation (8) into Equation (5) yields:

$$e_x = (1-\theta_{us}) \alpha k \rho_s D^{-\beta} \left( \frac{\rho_m}{\rho_s - \rho_m} \right)^\beta n^{3/5(\beta-1)} J^{7/10\beta+3/10} q_x^{3/5\beta+2/5} \quad (9)$$

Surface runoff is assumed to be generated uniformly in a hillslope so that:

$$q_x = q_e x \quad (10)$$

where  $q_e$  is the surface runoff rate ( $\text{m}\cdot\text{s}^{-1}$ ). Putting Equation (10) into Equation (9) leads to:

$$e_x = (1-\theta_{us}) \alpha k \rho_s D^{-\beta} \left( \frac{\rho_m}{\rho_s - \rho_m} \right)^\beta n^{3/5(\beta-1)} J^{7/10\beta+3/10} q_e^{3/5\beta+2/5} x^{3/5\beta+2/5} \quad (11)$$

In the area of a hillslope, the characteristics of soil and microtopography basically do not vary largely, thus the parameters  $k$  and  $\beta$  can be assumed constant with  $x$ . Moreover,  $\rho_m$  increases from the top to the bottom in a hillslope, and is determined by  $e_x$ . If an expression of  $\rho_m$  is put into Equation (11),  $e_x$  can not be solved out in a simple form. Erosion rate of a whole hillslope can be obtained by integrating Equation (11) along the slope and multiplying the result by the width of hillslope. The  $\rho_m$  is assumed constant for the integration, and the integrated result is:

$$E = B \cdot \int_0^L e_x dx = B \cdot \frac{5}{3\beta+7} (1-\theta_{us}) \alpha k \rho_s D^{-\beta} \left( \frac{\rho_m}{\rho_s - \rho_m} \right)^\beta n^{3/5(\beta-1)} \cdot J^{7/10\beta+3/10} q_e^{3/5\beta+2/5} L^{3/5\beta+7/5} = \frac{5}{3\beta+7} (1-\theta_{us}) \alpha k \rho_s D^{-\beta} \left( \frac{\rho_m}{\rho_s - \rho_m} \right)^\beta n^{3/5(\beta-1)} \cdot J^{7/10\beta+3/10} q_l^{3/5\beta+2/5} A \quad (12)$$

where  $E$  is the erosion rate of a hillslope ( $\text{kg}\cdot\text{s}^{-1}$ );  $B$  is the width of the hillslope (m);  $q_l$  is the runoff per meter width at the bottom of the hillslope ( $\text{m}^2\cdot\text{s}^{-1}$ ). The density of sediment laden flow,  $\rho_m$ , can be calculated by averaging the density of the clear flow at the top and that of the turbid flow at the bottom of the hillslope, because the actual range of the density of flow in a watershed is limited.

Equation (12) indicates that the erosion rate has an exponential relationship with surface discharge under given geometrical and physical parameters. The exponential terms in Equation (12) are determined by the parameter  $\beta$ ; and the coefficients are calculated with  $k$  and other physical parameters.

### 3. Physical Meanings of Parameters $k$ and $\beta$

In some popular soil erosion models, such as RUSLE in AnnAGNPS (Bingner et al., 2009), rainfall characteristics and soil erodibility are the main factors determining soil erosion amount, and microtopography is not directly considered. The WEPP model and ANSWERS-2000 take microtopography into consideration, but leave the rill space a tough problem for highly erodible regions. This paper intends to quantify microtopography by a parameter  $\beta$  in the proposed model. In this section, the physical meanings of parameters  $k$  and  $\beta$  are explained by experimental data (Xu et al., 1995a), so that the reasonability of the newly introduced parameter  $\beta$  can be validated.

In Xu's experiment, the artificial hillslope is 8 m wide and 10.5 m long on average by considering its fan-shaped toe. The

**Table 1.** Statistics of the Exponential Relationships Between  $q_l$  and  $E$  for Different Sets

Set	1	2	3	4	5	6	7	8	9	10
Exponent	0.77	1.08	1.37	0.51	1.30	1.33	1.12	1.58	1.32	1.35
R <sup>2</sup>	0.96	0.55	0.60	0.14	0.90	0.98	0.81	0.58	0.56	0.68

average gradient is 0.0638, and the median diameter of the loess particles is 0.076 mm. 10 artificial rainfall events with 90-minute duration and 0.0938 mm/s intensity were simulated with intervals from one to two days. Furthermore, the final landform of the previous rainfall event was used as the initial landform of a current rainfall event. As for the microtopography process, the tiny and shallow rills are considered as under development among the experimental sets 1 to 4; whereas, the rills are relatively stable among the following experimental sets (Xu et al., 1995b).

The amounts of runoff and soil erosion of each rainfall event are shown in Figure 3. Because of the sequential experiment design, the moisture content of soil increased dramatically at first, and then more slowly, which made runoff increased dramatically from Set 1 to Set 2, and then slightly. The erosion amount shows a tendency of firstly increase with runoff and then decrease, as in Figure 3. It is implied that the erosion amount is not only correlated to runoff, but is also affected by the development of hillslope microtopography. At the later stage of the experiment, the hillslope microtopography was fully developed so that soil erodibility decreased correspondingly; therefore, the amount of soil erosion could significantly decrease.

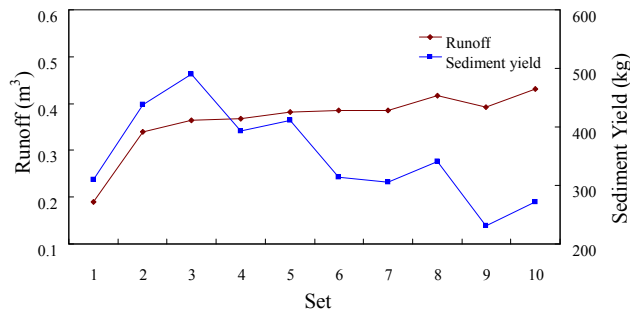


**Figure 3.** The sequences of runoff yield and erosion amount.

In a certain rainfall event, the values of  $k$  and  $\beta$  are supposed to be independent on time. Thus, the power of  $q_l$  in Equation (12) can be estimated by curve fitting with the experimental data as shown in Table 1. The majority of the erosion process is highly correlated to the corresponding runoff process except for the experimental set 4. In that set, the rills were in fast developing period caused by stochastic erosion events, and the erosion rate varied too dramatically to be accurately measured. Thus, that set will be omitted in the following discussion.

Values of the parameter  $\beta$  are calculated with the estimated values of the exponent of  $q_l$  in Equation (12); and values of the parameter  $k$  are fitted through using the least square method

according to Equation (12) with the experimental data. Since the value of  $\alpha$  can not be estimated separately from  $k$  in this study, it is assumed equal to 1. Those two parameters vary with the experimental sets as in Figure 4. The value of the parameter  $k$  dramatically decreases firstly, and then keeps relatively stable. The variation of  $k$  is consistent with that of the soil erodibility of the slope surface. At the beginning, the loose soil on surface could be detached easily; while lower layer soil became relatively more stable after hydraulic consolidating and coarsening at the later stage. Therefore, the parameter  $k$  is regarded as the nondimensional soil erodibility.

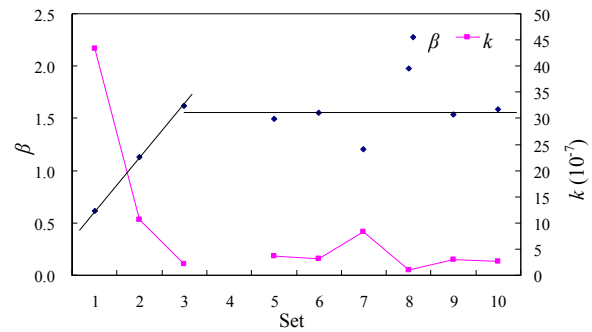


**Figure 4.** Variations of parameters  $k$  and  $\beta$  with experimental sets.

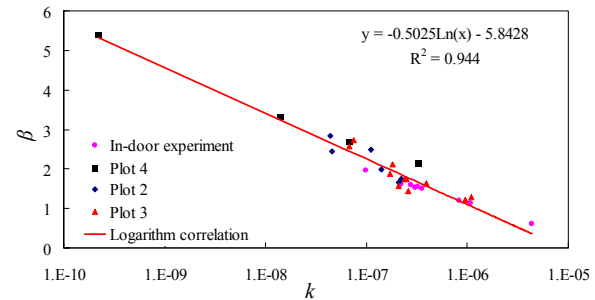


**Figure 5.** Pairs of  $k$  and  $\beta$  calibrated by using data from in-door experiment and field plots.

For the parameter  $\beta$ , it increases at the beginning and then vibrates within a relatively small range, which is consistent with the development of rills on the hillslope. This consistency implies that the eroding efficiency of surface runoff increases with the strengthened convergence of runoff due to the development of rills. Thus, for a certain soil type, the value of the parameter  $\beta$  mainly depends on the microtopography. When the microtopography is stable, the variation of the calibrated  $\beta$  is caused by random events such as collapse in rills. In general,

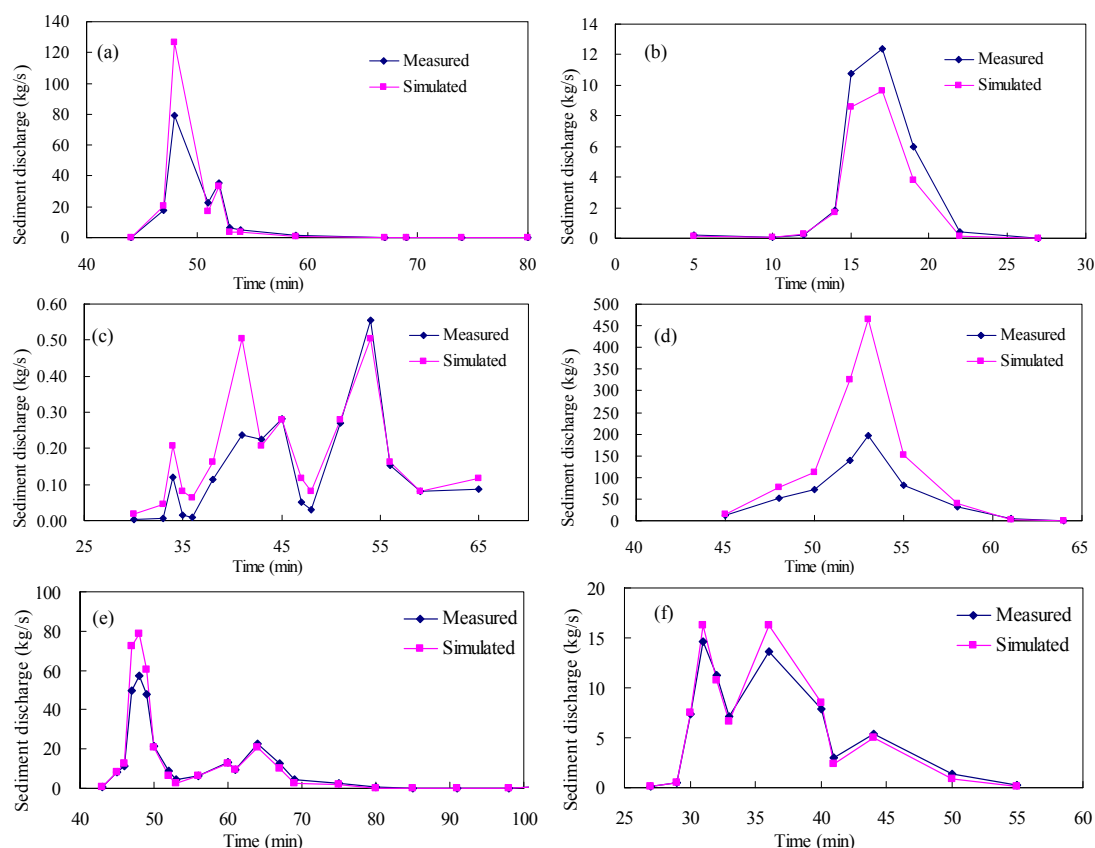


**Figure 6.** Soil erosion processes denoted by simulated and measured sediment discharges at the outlet of Plot 7: (a) August 22, 1967; (b) August 25, 1967; (c) August 26, 1967; (d) July 15, 1968; (e) July 25, 1968; and (f) August 22, 1968.

each parameter of  $k$  and  $\beta$  has its own physical meaning, which partly proves the reasonability of the developed hillslope soil erosion model.

#### 4. Validation and Application

##### 4.1. Validation in Field Plots

In this section, data from field plots are used to validate the proposed model. The Chabagou watershed, with an area of 205 km<sup>2</sup>, locates in a typical region of the gullied Loess Plateau. According to field measurements, the median size of soil particles is 0.08 mm approximately for the whole watershed. In the 1950s and 1960s, field observations of rainfall-runoff and soil erosion were carried out at experimental plots in the Chabagou watershed. Among the plots, Plot 4, 2, and 3 are rectangle hillslopes from hill top with the same gradient of 0.404, and with the lengths of 20m, 40m, and 60m respectively. Data from those plots in 1967 and 1968 are used to calibrate the parameters  $k$  and  $\beta$ . Measured runoffs and sediment concentrations are in the interval of 1 to 2 minutes. All rainfall-runoff events with more than 5 data points are chosen for parameter calibration respectively. Therefore, 21 sets of  $k$  and  $\beta$  are obtained, as plotted in Figure 5.

Figure 5 presents that parameter  $\beta$  is highly correlated to  $k$  in logarithm. The relation between  $\beta$  and  $k$  is also given in Figure 5. The correlation shows a stable connection between soil erodibility and microtopography under certain geographical and under-lying conditions. That is, larger  $\beta$  denoting high eroding efficiency of runoff usually occurs after the development of rills and tiny gullies. Accompanying with the development of microtopography, the soil erodibility  $k$  is decreased by the lost of incompact surface particles. The development of microtopography may cycle annually in farmland, because rills and tiny gullies are erased by tillage. However, the erosion parameters are more or less invariable in storm seasons in the studied region, since microtopography can fast evolve to a stable condition after only one or two rainstorms.

Observed data from Plot 7, a natural hillslope covering 5740 m<sup>2</sup>, is chosen to validate the developed erosion model. The equivalent length of the hillslope is 110 m, and the gradient of the 40% long and most mild segment at the bottom is 0.344. The average value of parameter  $k$  in Plot 3 (the longest one) is  $3.54 \times 10^{-7}$ , and  $\beta$  is 1.62 by using its relation with  $k$ . These values of  $k$  and  $\beta$  are used for Plot 7. All the observed data of rainstorms in 1967 and 1968 are used for the validation. Equation (12) is used in each time step with measured run-

off as the input. Simulated values at the outlet of Plot 7 are compared with measured values as shown in Figure 6. It is indicated that simulated soil erosion processes basically agree with measured processes. The errors of peak sediment discharge are less than 70% except for the most intensive rainstorm as in Figure 6(d). The model will be further tested in watersheds to check out whether the over estimation of soil erosion in heavy rainstorm is occasional, or systemic that caused by be the proposed model itself.

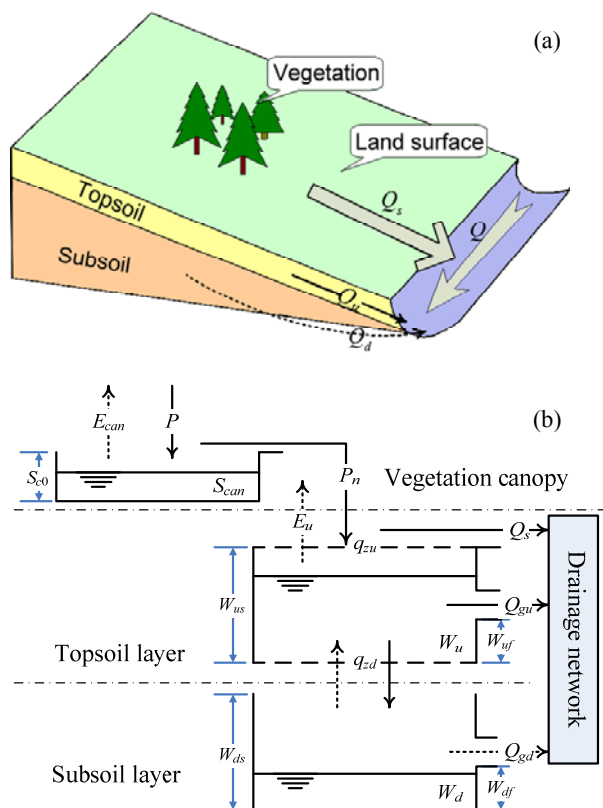


**Figure 7.** Schematics of hillslope rainfall-runoff simulation: (a) a conceptual hillslope (the soil is divided into two layers: topsoil and subsoil); (b) hydrological responses simulated in different layers.

#### 4.2. Integration in the DYRIM

The proposed model is integrated into the DYRIM so that continuous simulations of rainfall-runoff, soil erosion, and sediment transport in watersheds can be achieved. In the integrated model, at each time step rainfall-runoff is simulated firstly and then the results are taken as the input of the soil erosion model. Since hillslope runoffs are the input, the rainfall-runoff model is briefly introduced here.

The influence of ground water on hillslope surface runoff is ignored in this study, because the unsaturated zone of soil can be dozens of meters deep in the Loess Plateau. Hillslope soil is divided into two layers: topsoil and subsoil, as shown in Figure 7(a). The bottom of the topsoil layer is parallel to

the hillslope surface, and the subsoil layer is triangle shaped in the longitudinal cross-section view of the hillslope. Infiltration-excess flow is mainly considered in the model, along with related processes such as vegetation interception, evaporation, soil water flow, and water redistribution between the two soil layers. All simulated hydrological responses are shown in Figure 7(b).

The mass conservation equations of the canopy storage, topsoil water and subsoil water are:

$$\frac{\partial S_{can}}{\partial t} = P - P_n - E_{can} \quad (13.1)$$

$$\frac{\partial W_u}{\partial t} = A \cdot (q_{zu} - q_{zd} - E_u) - Q_{gu} \quad (13.2)$$

$$\frac{\partial W_d}{\partial t} = A \cdot q_{zd} - Q_{gd} \quad (13.3)$$

where  $S_{can}$  is the canopy storage (m),  $t$  is time (s),  $P$  is the rainfall intensity (m/s),  $P_n$  is the net rainfall intensity (m/s),  $E_{can}$  is the evaporation rate of canopy water (m/s),  $W_u$  is the water storage of topsoil(m<sup>3</sup>),  $q_{zu}$  is the infiltration rate of land surface (m/s),  $q_{zd}$  is the infiltration rate from topsoil to subsoil (m/s),  $E_u$  is the evaporation rate of topsoil water (m/s),  $Q_{gu}$  is topsoil drainage (m<sup>3</sup>/s),  $W_d$  is the water storage of subsoil (m<sup>3</sup>),  $Q_{gd}$  is subsoil drainage (m<sup>3</sup>/s).

The value of  $q_l$  to simulate the soil erosion process is calculated as:

$$q_l = (P_n - q_{zu}) \cdot L, \text{ when } P_n > q_{zu} \quad (14)$$

where  $P_n$  is the output of canopy layer simulated with the Kristensen-Jensen approach as in MIKE SHE WM (Vázquez and Feyen, 2003), and  $q_{zu}$  is the output of infiltration simulation of the topsoil layer as follows.

By assuming that the moisture content at the vertical middle of the topsoil layer equals to its average value, and the surface soil is saturated during rainfall, the infiltration process from the land surface to the topsoil is generalized as one-dimensional vertical seepage, where the unsaturated Darcy's law can be used. The relative hydraulic conductivity of unsaturated soil is expressed by an exponential function of the saturation degree. The pressure drop from the land surface to the middle of topsoil layer equals to the differences of the gravity and matric potentials. The matric potentials are estimated by using exponential function of the saturation degree of soil. Therefore, the variation of infiltration rate can be calculated with the volumetric water content of topsoil  $\theta_u$  as:

$$q_{zu} = K_{zus} \cdot \left( \frac{1 + \theta_u(t)/\theta_{us}}{2} \right)^{\beta_u} \left[ 1 + \frac{2a_u}{h_u} \left( \frac{\theta_u(t)}{\theta_{us}} \right)^{-b_u} \right] \quad (15)$$

where  $K_{z_{us}}$  is the saturated vertical hydraulic conductivity of the topsoil (m/s);  $\theta_{us}$  is the saturated volumetric water content of the topsoil ( $m^3/m^3$ ); exponent  $\beta_k$  is determined by the grain composition of soil;  $h_u$  is the thickness of the topsoil layer (m); and  $a_u$  (m) and  $b_u$  are the matric potential coefficients of the topsoil.

To calculate the variation of  $\theta_u$ , all the contributing processes are simulated. The redistribution of soil water, that is, the exchange of water between the topsoil and the subsoil layers, is calculated following the unsaturated soil hydrodynamics. Discharge from the topsoil layer is simulated using Darcy's law when its water content is greater than the soil storage capacity, though it merely happens in the Loess Plateau. Soil water evaporation is simulated with soil water content and potential evaporation by using the equation proposed by Fu (1981), in which the variation of soil water content in different stages is smoothly considered.

Simulated flow and sediment discharges of a hillslope are treated as direct inputs of subsequent models to simulate the movements of water and sediment in the river reach corresponding to that hillslope. Confluence and flow routing in the drainage network are simulated using a diffusive wave method, and non-equilibrium sediment transport is simulated using the method proposed by Fei and Shao (2004). Therefore, water and sediment movements in a whole watershed can be simulated with the DYRIM (Wang et al., 2007).



Figure 8. The drainage network of Chabagou watershed (extracted from 50 m × 50 m DEM).

### 4.3. Application in Watershed

The integrated model is applied to the Chabagou watershed. With the 50 m × 50 m resolution DEM, the watershed is delineated by 4,763 units (a river reach with 2 or 3 hillslopes) with an average hillslope area of 0.017 km<sup>2</sup>. The drainage network, rainfall stations and hydrological stations are shown in Figure 8. There are six hydrological stations and 31 rainfall stations.

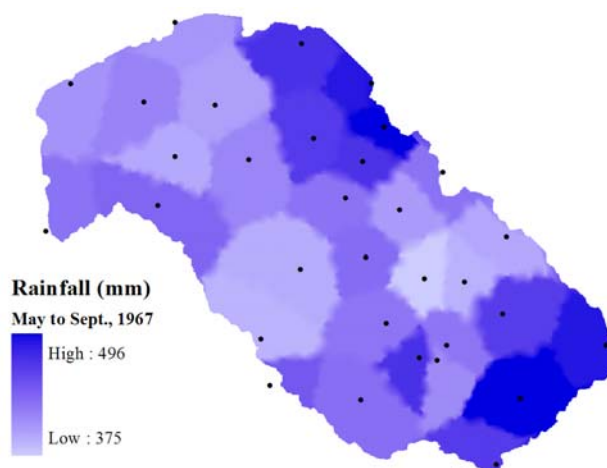


Figure 9. Distribution of precipitation in the simulated period in the Chabagou watershed.

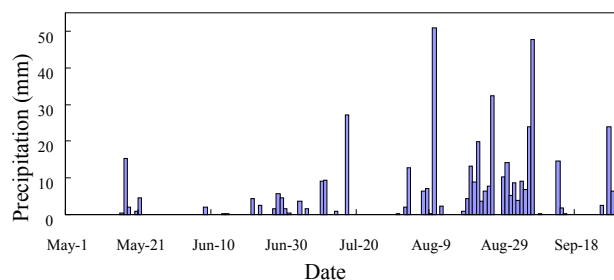


Figure 10. Daily precipitation of Caoping Station (a rain storm occurred in August 26 contributed to the maximum flood peak in that year).

Table 2. Statistics of Runoff Simulation in all the Hydrological Stations

Station	Drainage Area (km <sup>2</sup> )	Error of runoff (%)	Error of peak discharge (%)	NSE of discharge
Shejiagou	4.26	25.9	-3.5	0.35
Tuoxiang	5.74	-50.0	57.1	0.53
Sanchuankou	21.0	49.3	33.7	<0
Xizhuang	49.0	-14.2	0.2	0.73
Dujiagoucha	96.1	-28.0	1.0	0.89
Caoping	187	-3.6	-3.3	0.90

\* The flood peaks were all counted on August 26<sup>th</sup>.

Rainfall-runoff, soil erosion, and sediment transport processes in 1967 are simulated with precipitation data from those 31 rainfall stations. According to the recorded rainfall processes with time steps in the vicinity of 12 minutes, the time step for simulation is set as 6 minutes. The period from May to September in 1967 is selected as the period for rainfall-runoff calibration. The nearest neighbor method is adopted to spatially interpolate rainfalls so that the precipitation distribution is generated as shown in Figure 9. The daily precipitation at Caoping Station is shown in Figure 10 as an example.

Comparison of the observed and simulated discharges at Caoping Station, which is used for the optimization of rainfall-runoff parameters, is shown in Figure 11. The results of error analysis for runoff yields, flood peaks and the Nash-Sutcliffe coefficient of efficiency (NSE) of all the gauge stations are listed in Table 2. There are mainly two reasons resulting in the errors of runoff simulation, especially in small tributaries. One is that the recorded data of all rainfall stations are not in the same time interval; thus rainfall intensities are not spatially equally expressed. The other is that the spatial distribution of underlying parameters is not considered due to the lack of data.

**Table 3.** Statistics of Sediment Discharge Simulation in all the Hydrological Stations

Station	Measured sediment discharge (tons)	Simulated sediment discharge (tons)	Error of sediment discharge (%)	NSE of sediment concentration
Shejiagou	$5.57 \times 10^4$	$6.99 \times 10^4$	-7	0.69
Tuoerxiang	$7.53 \times 10^4$	$3.28 \times 10^4$	-41	0.35
Sanchuankou	$2.15 \times 10^5$	$4.21 \times 10^5$	96	0.43
Xizhuang	$9.08 \times 10^5$	$6.80 \times 10^5$	-25	0.63
Dujiagoucha	$2.32 \times 10^6$	$1.56 \times 10^6$	-33	0.76
Caoping	$3.64 \times 10^6$	$3.76 \times 10^6$	3	0.60

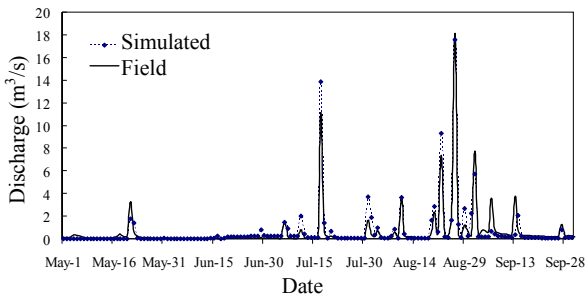


**Figure 11.** Comparison of field and simulated flow discharges at Caoping Station.

With the simulation results of hillslope runoff, soil erosion on hillslopes and non-equilibrium sediment transport in channels are further simulated by using the DYRIM. Gravitational erosion in gully slopes that also contributes to sediment discharge is also simulated using the module (Wang et al., 2005) in the DYRIM, which is introduced by Li et al. (2008). The parameters of  $k$  and  $\beta$  used in the hillslope erosion model are  $3.54 \times 10^{-7}$  and 1.62, respectively, same as those used in model validation in field Plot 7. The simulated sediment discharges and their NSEs at all stations are listed in Table 3. Most stations have NSE greater than 0.5. Sediment concentrations at four stations as shown in Figure 12 also indicate that the simulated and observed sediment discharges are in the same order of magnitude. The distribution of hillslope soil erosion in the whole watershed as shown in Figure 13 is consistent with the distributions of rainfall intensity and slope gradient in the watershed. The hillslope erosion modulus in several regions with high concentrated precipitation is larger than 20,000 tons /km<sup>2</sup>.

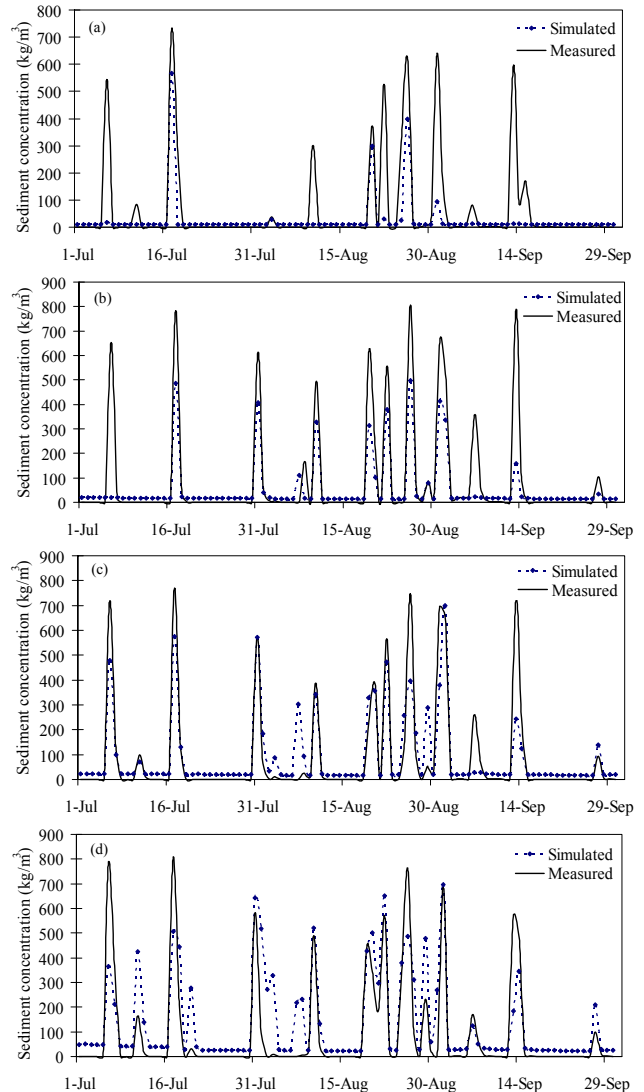


**Figure 12.** The comparison of measured and simulated sediment concentrations: (a) Tuoerxiang, (b) Xizhuang, (c) Dujiagoucha, and (d) Caoping.

With hillslope soil erosion as the main source of sediment, the integrated model DYRIM is notably effective in simulating the whole processes of rainfall-runoff, soil erosion, and sediment transport in watersheds. In the continuum of simulation, the proposed hillslope erosion model plays a critical role. Soil erosion simulation with the same time step as that in hydrological and hydro-dynamical models can maintain the continuity of the simulations of those dynamical processes. Therefore, detailed sediment-graphs can be simulated from measured or forecasted rainfall inputs rather than upstream sediment-graphs. The developed soil erosion model helps to advance traditional sediment transport model for river channels to an integrated system with hydrological model that covers a whole river basin.



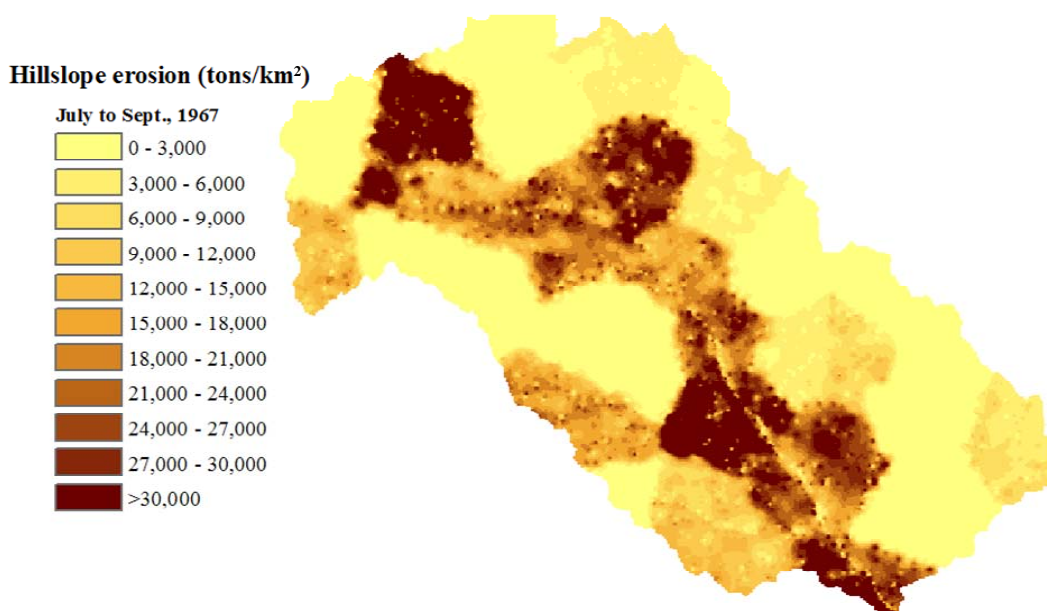


**Figure 13.** Distribution of hillslope erosion in Chabagou watershed shows its correlation with rainfall intensity and hillslope gradient.

However, distributed simulation of rain-runoff is difficult in arid and semi-arid areas due to remarkable variations of infiltration rate and soil moisture. The simulation of soil erosion process in this paper is based on the rain-runoff simulation results that inevitably bring errors into soil erosion simulation. This is approved by the fact that most of the simulation errors of sediment discharge and flow discharge have the same tendencies. Moreover, errors from the simulations of gravitational erosion, flow routing and sediment transport also contribute to the errors of simulated sediment concentrations. Therefore, the simulation accuracy of sediment discharge depends on all the modules of water and sediment movement processes and their hybrids in a watershed.

In this paper, the two key parameters of developed model are estimated from a few field plots experiments, thus they are only valid and suitable for watersheds with similar soil property of loess and land surface with sparse vegetation and numerous rills.

### 5. Conclusions

In this paper, splash erosion, sheet erosion and rill erosion are generalized as a unified process of hillslope soil erosion. To simulate this process, a model taking surface runoff as its input is developed. Two dimensionless parameters are proposed, namely the parameter  $k$  that presents soil erodibility and parameter  $\beta$  that reflects the effect of microtopography on the confluence of runoff, respectively. They are proved reasonable by using indoor experimental data.

The developed model is validated using measured data from field plots. The model is integrated into the DYRIM, and

is applied to simulate soil erosion processes in the Chabagou watershed. The results indicate that the developed model can reasonably simulate soil erosion processes in the Loess Plateau.

After integrating all relevant models, the DYRIM can simulate all hydrological and sediment processes in a river basin to facilitate the investigation of soil erosion and sediment runoffs. Since the simulated process of hillslope erosion is in the time step short enough to dynamically simulate the hyper-concentrated sediment laden flow in river channels, the erosion model proposed in this paper plays a crucial part in building up the whole modeling system.

Future research efforts can be made in (a) identifying typical values of parameters  $k$  and  $\beta$  for different soil textures and microtopographies, (b) investigating the impacts of vegetation, land use and soil water conservation measures on parameters  $k$  and  $\beta$ , and (c) verifying whether the proposed model has scale effect problems and making efforts to achieve a scale-independent version.

**Acknowledgments.** The authors wish to acknowledge the projects of the National Key Basic Research Program of China (Grant No. 2005CB724200 and 2007CB714100), and the Chinese Postdoctoral Science Foundation (Grant No. 20080440392) for their partially financial support of this work.

### References

Bingner, R.L., Theurer, F.D., and Yuan, Y. (2009). AnnAGNPS Technical Processes Documentation, Version 5.0, USDA-ARS National Sedimentation Laboratory. [ftp://199.133.90.201/pub/outgoing/AGNPS/AGNPS\\_Web\\_Files/pdf\\_files/AnnAGNPS\\_Techni](ftp://199.133.90.201/pub/outgoing/AGNPS/AGNPS_Web_Files/pdf_files/AnnAGNPS_Techni)

- cal\_Documentation.pdf.
- Cai, Q., Liu, J., and Liu, Q. (2004). Research of sediment yield statistical model for single rainstorm in Chabagou drainage basin, *Geographical Research*, 23(4), 433-439.
- Cao, Z., Pender, G., and Meng, J. (2006). Explicit formulation of the Shields diagram for incipient motion of sediment, *J. Hydraul. Eng.*, 132(10), 1097-1099, doi:10.1061/(ASCE)0733-9429(2006)132:10(1097).
- Dabral, S., and Cohen, M. (2001). ANSWERS-2000: Areal Non-point Source Watershed Environmental Response Simulation, <http://www.agen.ufl.edu/~klc/abe6254/answers01.pdf>.
- Fei, X., and Shao X. (2004). Sediment transport capacity of gullies in small watersheds, *Journal of Sediment Research*, (1), 1-8.
- Flangan, D.C., and Nearing, M.A. (ed.) (1995). *USDA - Water Erosion Prediction Project: Hillslope Profile and Watershed Model Documentation*, USDA-ARS, NSERL, Report no.10. USDA-ARS, Indiana, USA, <http://www.ars.usda.gov/Research/docs.htm?Docid=18073>.
- Foster, G.R., and Meyer, L.D. (1972). Transport of particles by shallow flow, *Trans. ASAE*, 15(1), 99-102.
- Fu, B. (1981). On the calculation of evaporation from soil, *Acta Meteorologica Sinica*, 39(2), 226-236.
- Knisel, W.G. (ed.) (1980). *CREAMS: A Field-scale Model for Chemicals, Runoff and Erosion from Agricultural Management Systems*, USDA Conservation Research report No. 26, USDA-ARS, Washington DC, USA.
- Li, T. (2008). *Mechanism and simulation of river basin sediment dynamics*, PhD dissertation, Beijing: Tsinghua University.
- Li, T., Wang, G., Zhang, C., and Xue, H. (2008). Simulation of gravitational erosion in river basins on Loess Plateau, *Journal of Tianjin University*, 41(9), 1136-1141.
- Li, T., Wang, G., and Chen, J. (2009). Structural codification of drainage networks, *Comp. & Geosci.*, submitted.
- Li, Z., Fun, S., Xie, J., and Ruan, B. (1998). A study on storm runoff sediment yield in Kuyehe river watershed, *J. Hydraul. Eng.*, (Supplement), 18-23.
- Vázquez, R.F., and Feyen, J. (2003). Effect of potential evapotranspiration estimates on effective parameters and performance of the MIKE SHE-code applied to a medium-size catchment, *J. Hydrol.*, 270(3-4), 309-327, doi:10.1016/S0022-1694(02)00308-6.
- Wang, G., Wu, B., and Li, T. (2007). Digital Yellow River Model, *Journal of Hydro-Environment Research*, 1(1), 1-11.
- Wang, G., Xue, H., and Li, T. (2005). Mechanical model for gravitational erosion in gully area, *Journal of Basic Science and Engineering*, 13(4), 335-344.
- Xu, W., Ni, J., Xu, H., and Jin, D. (1995a). Experimental study on erosion process over loess slopes: I, *Journal of Soil and Water Conservation*, 9(3), 9-18.
- Xu, W., Ni, J., Xu, H., and Jin, D. (1995b). Experimental study on erosion process over loess slopes: II, *Journal of Soil and Water Conservation*, 9(3), 19-28.